Appl Phys A (2008) 92: 615–620
DOI 10.1007/s00339-008-4546-7

**Applied Physics A**
**Materials Science & Processing**

# Self-cleaning characteristics on a thin-film surface with nanotube arrays of anodic titanium oxide

**Chien-Chon Chen · Jin-Shyong Lin · Eric Wei-Guang Diau · Tzeng-Feng Liu**

Received: 15 January 2008 / Accepted: 17 April 2008 / Published online: 15 May 2008


**Abstract** Self-cleaning of a surface of nanotube arrays of anodic titanium oxide (ATO) is demonstrated. The ATO was prepared in fluoride ion containing sulfate electrolytes with a structure of 0.4 μm length, 100 nm pores diameter, 120 nm interpore distance, 25 nm pore wall thickness, a $8 \times 10^9$ pores $cm^{-2}$ pore density, and 68.2% porosity. Prepared as thin films either directly from a Ti foil or on a glass substrate, these arrays have the property that water drops spread quickly over the surface of the films without irradiation. In contrast, a flat anatase $TiO_2$ film requires irradiation with UV light for several minutes before the contact angle decreases to zero. The observed self-cleaning behavior of the ATO thin films is due to the capillary effect of the nanochannel structure and the superhydrophilic property of the anatase $TiO_2$ surface inside the tube.

**PACS** 96.15.Lb · 61.46.-W · 61.46.Fg

## 1 Introduction

From ancient times rutile titania ($TiO_2$) has had a common use as a white pigment because it is economical, chemically stable, and harmless [1], but anatase $TiO_2$ becomes active under irradiation with ultraviolet (UV) light. This characteristic has been extensively applied for self-cleaning, antifogging, antibacterial activity [2], conversion of solar energy [3], splitting of water [4], and storage of energy [5–8]. When $TiO_2$ is illuminated with UV light, a photocatalytic effect occurs on the $TiO_2$ surface such that the contact angle at the boundary between $TiO_2$ and $H_2O$ decreases to zero. Surfaces that are rough on a nanoscale tend to be more hydrophobic than smooth surfaces because of the reduced contact area between the water and solid. The nanoscale roughness is also essential to the self-cleaning effect—on a smooth hydrophobic surface, water droplets slide rather than roll. It has been demonstrated that the nanoscale surface roughness causes superhydrophobicity. This prevents wetting, causes such a surface to suspend small liquid droplets, and causes the contact angle to approach 180° leading to almost spherical droplets. If such droplets had a chance to solidify, then they would be likely to form solid spherical particles. From Patankar's [9] simulation, the contact angle of a drop is a function of the roughness of a solid surface and is described by the equation, $(H/W) > -(1+\cos\theta)/2\cos\theta$, where $\theta$ is the contact angle between the liquid and solid, $H$ is the height and $W$ is the width of the groove. Also, Cassie's analysis [10] for a porous surface of heterogeneous surfaces states that $\cos\theta'' = \sigma_1 \cos\theta - \sigma_2$, where $\theta''$ is the contact angle, $\sigma_1$ is the solid surface area, and $\sigma_2$ represents air spaces. The rate of hydrophilic conversion depends on the experimental conditions; for example, this rate increases with increased intensity of UV light, a decreased UV wavelength, and an increased period of UV illumination [11]. The control of surface wettability induced by argon-ion ($Ar^+$) [12], iron-ions ($Fe^{3+}$) [13] sputtering, and surface modified by octadodecyldimethylchlorosilane (ODS) [14] have also been observed on thin films of $TiO_2$. A self-cleaning surface occurs when the contact angle between a liquid and solid

C.-C. Chen · E.W.-G. Diau (✉)
Department of Applied Chemistry and Institute of Molecular Science, National Chiao Tung University, Hsinchu, Taiwan 30010, Taiwan
e-mail: diau@mail.nctu.edu.tw

J.-S. Lin · T.-F. Liu
Department of Material Science and Engineering, National Chiao Tung University, Hsinchu, Taiwan 30010, Taiwan

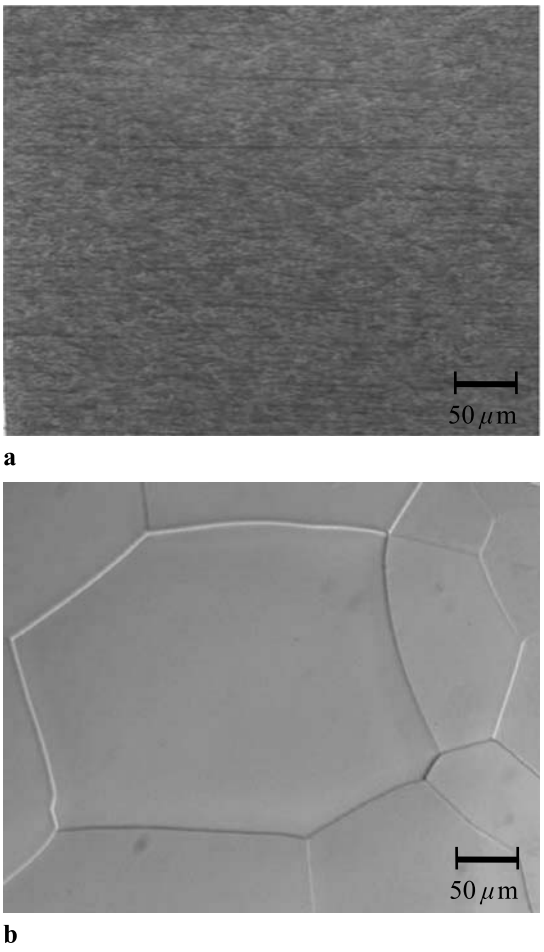


**Fig. 1** Optical microscope images of a titanium surface after (**a**) mechanical polishing and (**b**) electrolytic polishing

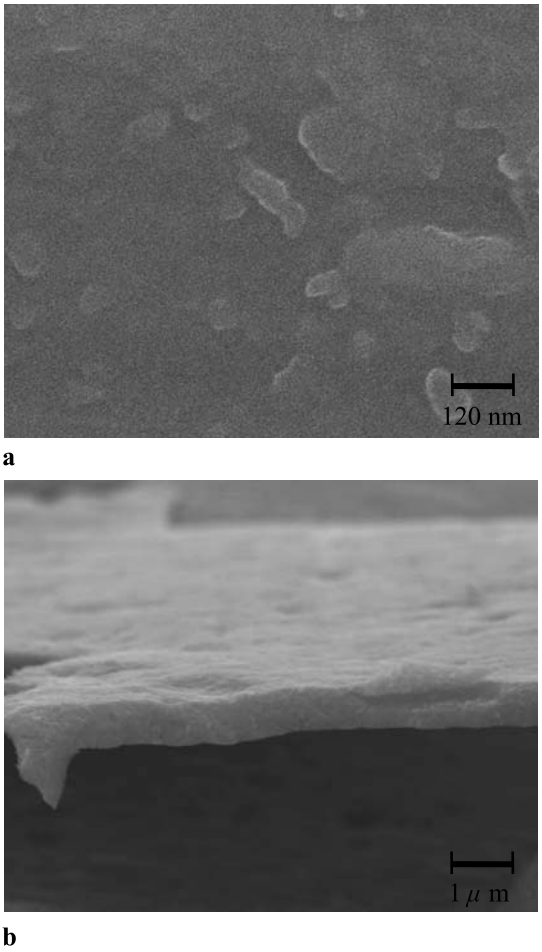


**Fig. 2** SEM images of a $TiO_2$ thin film produced on annealing (sample 1): (**a**) a top view shows the compact $TiO_2$ film; (**b**) a cross-section view shows the film thickness 900 nm

is near 0° or 180°. For instance, water forms a drop (180°) on a lotus leaf (a hydrophobic or lotus effect) or forms a thin aqueous film (so zero angle) on anatase $TiO_2$ (a hydrophilic effect). Because a contact angle at 0° or 180° impedes the retention of water on the solid surface, the water slides from the solid, removing dust. According to Young's equation [15],

$$\gamma_L \cos\theta = \gamma_S - \gamma_{SL}, \tag{1}$$

the contact angle $\theta$ is related to the surface tension $\gamma_L$ of the liquid, the surface tension $\gamma_S$ of the solid and the surface tension $\gamma_{SL}$ between the liquid and solid. According to Girifalco and Good [16], the latter quantity is expressible as

$$\gamma_{SL} = \gamma_S + \gamma_L - \phi(\gamma_S/\gamma_L)^{0.5}, \tag{2}$$

in which $\phi$ is a constant (typically in a range 0.6–1.1). From (1) and (2), the cosine of the contact angle becomes expressed as

$$\cos\theta = C\sqrt{\gamma_S} - 1 \tag{3}$$

in which $C$ is a constant. An increased surface tension on the solid hence causes a decreased contact angle so that the solid tends to become hydrophilic.

The roughness of a solid surface also affects the contact angle. A rough hydrophilic surface tends to be more hydrophilic, whereas a rough hydrophobic surface tends to be more hydrophobic than the corresponding smooth surfaces [17, 18]. Because $TiO_2$ is a hydrophilic material, roughening the surface of a porous $TiO_2$ film causes it to become superhydrophilic. Balaur et al. [19, 20] demonstrated the wettability of a $TiO_2$ film with a nanotubular structure modified by self-assembled organic monolayers. Through illumination with a UV light, the wetting properties of a $TiO_2$ surface are thus controllable from superhydrophobic to superhydrophilic [19].

In the present work, we demonstrate that self-cleaning is achieved with a structure of nanotube arrays of anodic titanium oxide (ATO) on the surface of thin films of anatase $TiO_2$. We find that the ATO nanostructural films display a superhydrophilic property such that water drops spread

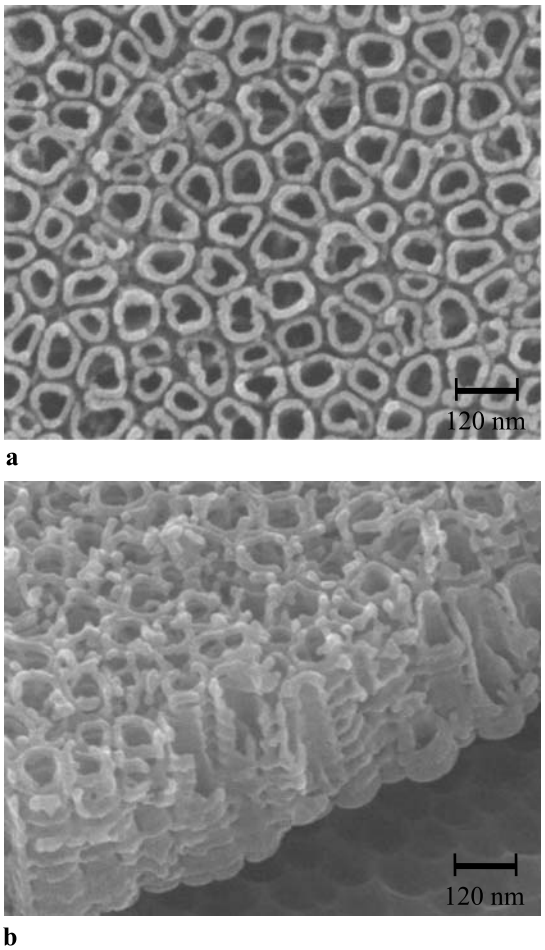


**Fig. 3** SEM images of a $TiO_2$ thin film on a Ti-foil substrate (sample 2): (**a**) a top view shows the nanochannel structure; (**b**) a cross-section view shows the film thickness 400 nm. The film was produced on anodization in HF (0.5 vol.%) + $H_2SO_4$ (10 vol.%) electrolyte

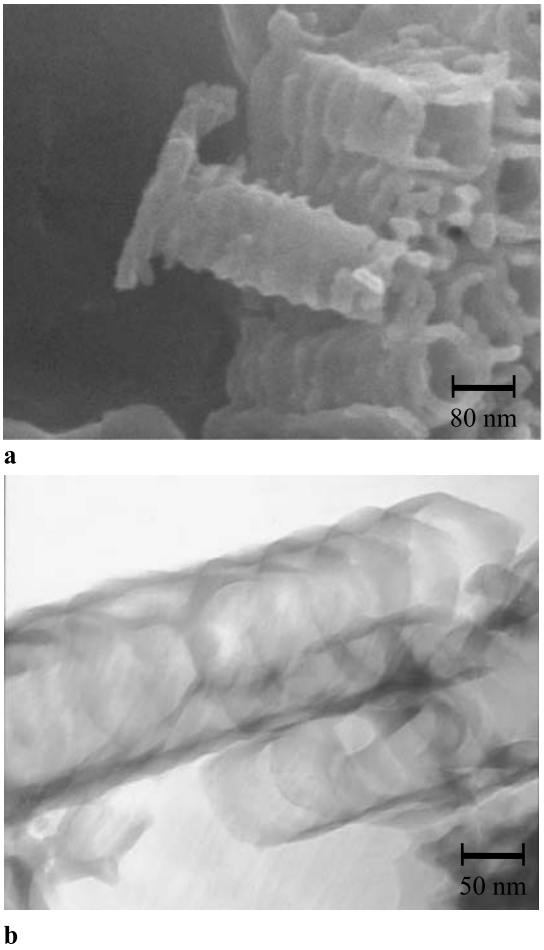


**Fig. 4** Enlarged (**a**) SEM and (**b**) TEM images showing the ring-packed nanotube structure of sample 2

quickly over the ATO surface without illumination. In contrast, for compact anatase $TiO_2$ films, the contact angle decreases to zero after UV radiation was applied on the surface for several minutes.

## 2 Experiments

To fabricate $TiO_2$ films we used titanium substrates of three types: sample 1 was a titanium plate (purity 99.995%, thickness 10 mm), sample 2 was a commercial titanium foil (purity 99.7%, thickness 0.127 mm), and sample 3 was a thin film of titanium (purity 99.995%, thickness 500 nm) formed on a glass substrate by sputtering. The area of each titanium substrate was 2 cm × 2 cm. To obtain a homogeneous $\alpha$-Ti structure, we annealed samples 1 and 2 in an air furnace for 1 h, whereas sample 3 was annealed in an evacuated chamber ($P < 10^{-4}$ Pa). The annealing temperature was controlled below the temperature of the $\beta$-phase transformation at 850°C. For samples 1 and 2, a clean and flat surface was obtained on mechanical and electrolytic polishing; the electrolytic polishing involved a platinum sheet (2 cm × 2 cm) as a cathode, titanium plates as an anode, perchloric acid ($HClO_4$, 5 vol.%, 70%) + ethandiol monobutylether ($HOCH_2CH_2OC_4H_9$, 53 vol.%, 95%) + methanol ($H_3COH$, 42 vol.%, 99%) as an electrolyte at 15°C, with 52 V applied for 1 min followed by 28 V for 13 min, and with constant stirring at 200 rpm.

After a clean and plate-shaped $\alpha$-Ti surface was formed, a compact anatase $TiO_2$ film resulted from heating sample 1 to 450°C for 3 h in air in a furnace. The nanoporous $TiO_2$ films were formed on anodization followed by annealing at 450°C for 3 h. Sample 2 was anodized with hydrofluoric acid (HF, 0.5 vol.%, 55%) + sulfuric acid ($H_2SO_4$, 10 vol.%, 98%) electrolyte at 25°C, with 20 V applied for 10 min. Sample 3 was anodized with HF (0.15 vol.%) + $H_2SO_4$ (10 vol.%) electrolyte at 2°C, with 10 V applied for 1 min.

The micromorphology of the $\alpha$-Ti and $TiO_2$ surfaces was determined with an optical microscope (OM, Olym-

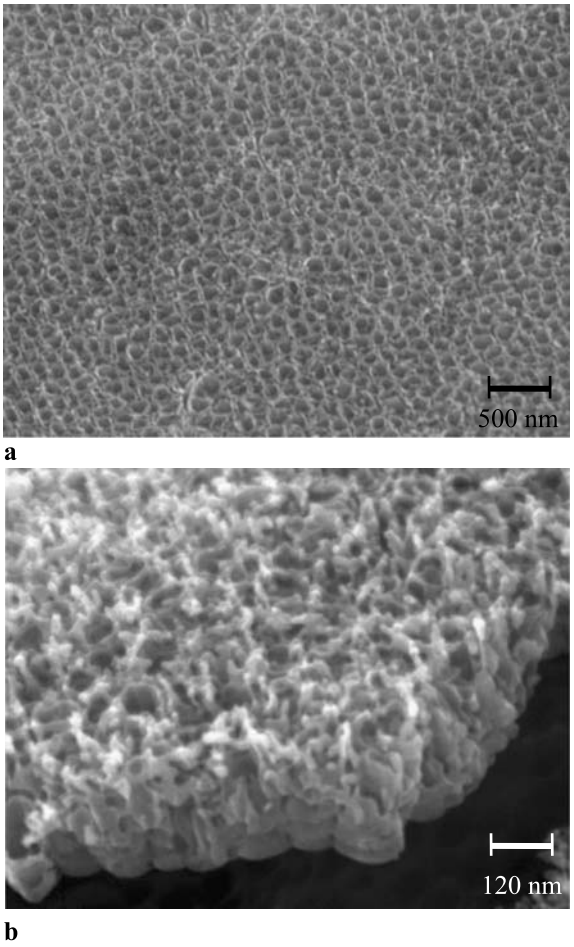


**Fig. 5** SEM images of a $TiO_2$ thin film on a glass substrate (sample 3): (**a**) a top view shows the nanoporous structure; (**b**) a cross-section view shows the film thickness 200 nm. The film was produced on anodization in HF (0.15 vol.%) + $H_2SO_4$ (10 vol.%) electrolyte

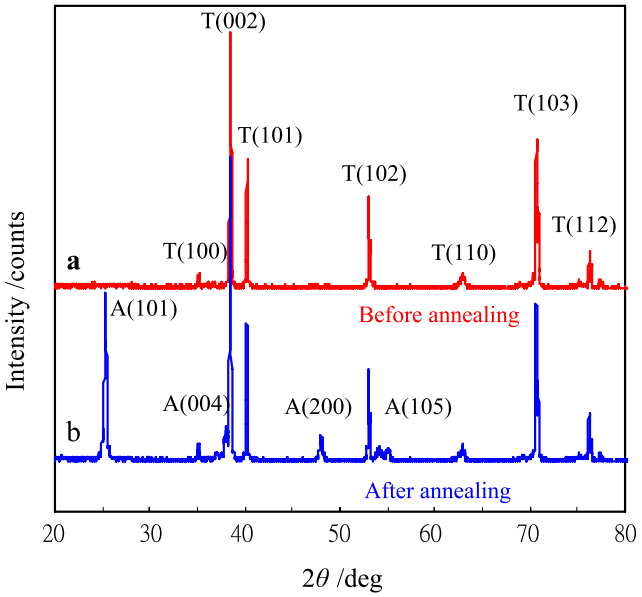


**Fig. 6** XRD patterns of a $TiO_2$ thin film with an ATO nanochannel structure on Ti foil (sample 2): (**a**) before annealing, the features show only an $\alpha$-Ti phase ($TiO_2$ is amorphous); (**b**) after annealing at 450°C for 3 h, the features show both the $\alpha$-Ti phase and an anatase $TiO_2$ phase. T and A represent titanium metal and anatase $TiO_2$, respectively

pus BJ-51), a scanning electron microscope (SEM, JEOL 6500, operating voltage 15 kV), and a transmission electron microscope (TEM, JEOL 2000, operating voltage 200 kV). For SEM images, the surface morphology of the ATO films was observed directly; for TEM images, the ATO films were scraped and collected on carbon/formvar films supported by Cu grids. The anatase $TiO_2$ was detected with X-ray diffraction (XRD, Philips X'Pert Pro, solid-state detection using filtered Cu $K\alpha$ radiation). The contact angle of $H_2O$ on the $TiO_2$ surface was determined in an equilibrium condition with a contact-angle meter (Phoenix 600) at 25°C. Optical images were obtained with a CCD camera interfaced to a computer; the contact angle was evaluated according to the equipment program.

## 3 Results and discussion

Figures 1a and 1b present optical micrographs of an $\alpha$-Ti surface after mechanical and electrolytic polishing, respectively. The ductility of titanium made it difficult to obtain a non-scraped surface by mechanical polishing alone. Figure 1a shows that an $\alpha$-Ti surface retains scrapes even after grinding with SiC paper (#4000) and polishing with $Al_2O_3$ powder (50 nm), whereas Fig. 1b shows that electrolytic polishing produces a non-scraped surface. Such a surface would form a $TiO_2$ film of high quality. If left in air near 23°C, a surface of titanium metal is known to become spontaneously covered with a transparent film of titania of thickness 1–10 nm. The thickness of the film is increased on either anodization or annealing. Figure 2 shows the results of annealing sample 1 for a compact $TiO_2$ film (thickness 900 nm) produced on the Ti plate after annealing at 450°C for 3 h.

For sample 2, Fig. 3 presents SEM images of ATO nanotube arrays on a Ti foil that was anodized in HF (0.5 vol.%) + $H_2SO_4$ (10 vol.%) electrolyte. The long-range ordered nanochannel structure has a length 400 nm, pores of diameter 100 nm, an interpore distance 120 nm, a pore wall of thickness 25 nm, a pore density $8 \times 10^9$ pores $cm^{-2}$, and a porosity 68.2%. Detailed images of ATO nanotubes of sample 2 appear in Fig. 4. The SEM (Fig. 4a) and TEM (Fig. 4b) images reveal the ring-packed structure for the ATO nanotubes. During anodization of Ti, the gases $TiF_{(g)}$, $TiF_{2(g)}$, $TiF_{3(g)}$, $TiF_{4(g)}$, $TiOF_{(g)}$ and $TiOF_{2(g)}$ are formed in the Ti–F–O electrochemical system [21, 22]. When the titanium is anodized, these gases and $H_{2(g)}$ escape from the titanium substrate through the titania film, leaving nanopores and forming an ATO nanochannel structure.

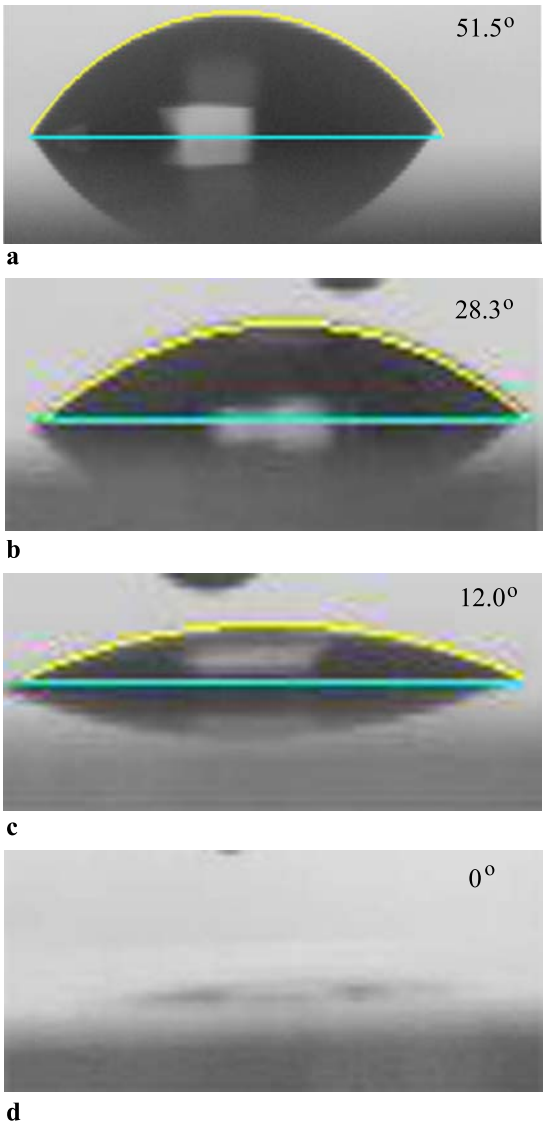


**Fig. 7** A water drop on the surface of a compact thin film of $TiO_2$ (sample 1) after ultraviolet illumination (350 nm, 2 mW cm$^{-2}$) for (**a**) 0, (**b**) 1, (**c**) 6, and (**d**) 20 min; the contact angles are 51.5°, 28.3°, 12° and 0°, respectively

Figure 5 shows images resulting from sample 3, which had pore size 40 nm and tube length 200 nm. The ATO nanostructures were formed on the glass substrate. To prevent the ATO thin film from flaking off the glass substrate, we controlled the HF concentration, electrolyte temperature, applied voltage and the duration of anodization to be significantly smaller than those conditions for sample 2. As a result, the surface morphology of the former (Fig. 5) was poorer than that of the latter (Fig. 3).

Figure 6 shows XRD patterns of sample 2, a large-scale $TiO_2$ thin film with ATO nanotubes on a Ti foil. Before annealing, the feature (denoted T) in Fig. 6a indicates the presence of only the $\alpha$-Ti phase ($TiO_2$ is amorphous); after the specimen was annealed at 450°C for 3 h, the XRD patterns

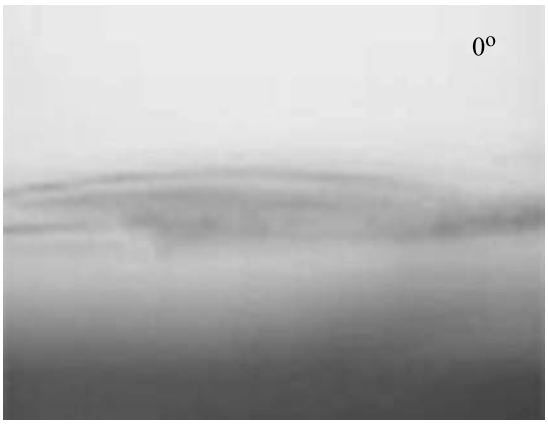


**Fig. 8** A water drop on the surface of a thin film of $TiO_2$ (sample 2) with ATO nanochannel arrays showing zero contact angle without ultraviolet illumination

shown in Fig. 6b reveal both the $\alpha$-Ti phase (denoted T) and the anatase $TiO_2$ phase (denoted A).

To determine the contact angle at the interface between the $TiO_2$ and $H_2O$, we placed a drop of $H_2O$ on the surface of $TiO_2$ films. Figure 7a shows that the initial contact angle of sample 1 was 51.5°. After ultraviolet illumination (350 nm, 2 mW cm$^{-2}$) for 1 min and 6 min, these angles decreased to 28.3° and 12.0°, respectively, as shown in Fig. 7b and 7c. With the duration of illumination increased to 20 min, the contact angle decreased to zero, as shown in Fig. 7d.

For both samples 2 and 3 for which ATO nanochannel arrays were produced on a Ti foil and a glass surface, the contact angles between $TiO_2$ and $H_2O$ were zero without ultraviolet illumination, as shown in Fig. 8. The observation of zero contact angle is rationalized according to a capillary effect, for which the height of the liquid inside the tube is expressible as [23]

$$h = (2\gamma \cos\theta)/(\rho g r) \tag{4}$$

in which appear symbols for liquid-air surface tension $\gamma$, contact angle $\theta$, density $\rho$ of liquid, acceleration $g$ due to gravity, and radius $r$ of the tube. For $H_2O$, values of these parameters are $\gamma = 0.072\,\mathrm{J\,m^{-2}}$, $\theta = 20°$, $\rho = 997\,\mathrm{kg\,m^{-3}}$, and $g = 9.8\,\mathrm{m\,s^{-2}}$. For a tube of diameter 100 nm ($r = 50$ nm), the height $h$ of a liquid column is estimated to be 280 m; $H_2O$ therefore becomes readily adsorbed inside these $TiO_2$ pores.

## 4 Conclusion

When the surface of a compact anatase $TiO_2$ film with water drops was irradiated with UV light (350 nm, 2 mW cm$^{-2}$) for 20 min, the contact angle of water on the surface decreased from 51.5° to zero, but the contact angle became

zero immediately when water drops were placed on an ATO nanochannel surface without UV light illumination. The ordered ATO nanostructural thin films with a great surface area exhibit a superhydrophilic nature as a prospective material for self-cleaning applications with beneficial properties of being robust, economical, chemically stable, transparent, and harmless.

**Acknowledgements** National Science Council of Republic of China (contract 96-2628-M-009-018-MY2) and the MOE-ATU program provided financial support.

## References

1. K. Hashimoto, H. Irie, A. Fujishima, Jpn. J. Appl. Phys. **44**, 8629 (2005)
2. K. Sunada, T. Watanabe, K. Hashimoto, Environ. Sci. Technol. **37**, 4785 (2003)
3. M. Grätzel, Nature **414**, 338 (2001)
4. A. Fujishima, K. Honda, Nature **238**, 37 (1972)
5. K.C. Chang, A. Heller, B. Schwartz, S. Menezes, B. Miller, Science **196**, 1097 (1977)
6. S. Licht, D. Peramunage, Nature **345**, 330 (1990)
7. M. Grätzel, Nature **414**, 338 (2001)
8. A.J. Nozik, R. Memming, J. Phys. Chem. **100**, 13061 (1996)
9. N.A. Patankar, Y. Chen, in *Tech. Proceedings of the 2002 Inter. Conf. on Modeling and Simulation of Microsystems*, U.S.A., 2002, p. 116
10. S. Baxter, A.B.D. Cassie, J. Text. Inst. **T46**, 36 (1945)
11. N. Sakai, A. Fujishima, T. Watanabe, K. Hashimoto, J. Phys. Chem. B **107**, 1028 (2003)
12. H. Irie, K. Hashimoto, Photocatalysis **15**, 78 (2004)
13. H. Jiang, L. Gao, Mater. Chem. Phys. **77**, 878 (2002)
14. X.T. Zhang, O. Sato, M. Taguchi, Y. Einaga, T. Murakami, A. Fujishima, Chem. Mater. **17**, 697 (2005)
15. P.C. Hiemenz, *Principles of Colloid and Surface Chemistry* (Dekker, New York, 1986). p. 37
16. L.A. Girifalco, R.J. Good, J. Phys. Chem. **61**, 904 (1957)
17. Z.-Z. Gu, A. Fujishima, O. Sato, Appl. Phys. Lett. **85**, 5067 (2004)
18. X.-T. Zhang, O. Sato, M. Taguchi, Y. Einaga, T. Murakami, A. Fujishima, Chem. Mater. **17**, 696 (2005)
19. E. Balaur, J.M. Macak, L. Taveira, P. Schmuki, Electrochem. Commun. **7**, 1066 (2005)
20. E. Balaur, J.M. Macak, H. Tsuchiya, P. Schmuki, J. Mater. Chem. **15**, 4488 (2005)
21. I. Barin, *Thermochemical Data of Pure Substances* (VCH Publishing, Weinheim, 1989)
22. J.L. Murray, *Phase Diagrams of Binary Titanium Alloys* (ASM International, Metals Park, 1987). p. 211
23. T. Engel, P. Reid, *Physical Chemistry* (Pearson Education, San Francisco, 2006). p. 184